

GEONEUTRINO OSCILLATIONS APPROACH TO
DISCRIMINATE DISTRIBUTIONS OF HPE IN
THE EARTH'S MANTLE USING THE MONTE
CARLO TECHNIQUE.

DANIEL FELIPE FORERO SÁNCHEZ

ADVISOR: JUAN CARLOS SANABRIA PhD.

This dissertation is submitted for the degree of
PHYSICIST



Physics Department
Faculty of Science
Universidad de Los Andes
Bogotá, Colombia
November 3, 2017

Dedicated to my little niece, Ana María, without whom this thesis would have been finished much, much earlier.

Contents

1	Introduction	2
2	Relevance of the Study	4
3	Distribution of Radioactive Elements	5
3.1	Distribution of Elements	5
3.2	Relative Abundances	6
3.2.1	Bulk Silicate Earth	6
3.2.2	Crust	7
3.2.3	Mantle	7
4	Radioactivity	9
4.1	Overview	9
4.2	Types of radioactive decay	10
4.2.1	Alpha decay	10
4.2.2	Gamma decay	10
4.2.3	Beta decay	10
4.3	Decay Chains	12
4.4	(Anti)Neutrino emission	13
5	Neutrino Physics	14
5.1	Time evolution	15
5.1.1	Three-flavor exact	15
5.1.2	Two-flavor approximation	16
6	The Model	18
6.1	Modelling the Earth	18
6.2	Modelling the Flux	18
6.2.1	The Flux Integral	18
6.2.2	Survival Probability	19
7	Results	21
8	Analysis	22

CONTENTS

v

9 Further Problems	23
10 Conclusions	24
References	25

List of Figures

4.1	Feynman diagram for β^+ process.	11
4.2	Feynman diagram for β^- process.	11
4.3	Feynman diagram for electron capture.	12
4.4	Geoneutrino energy spectrum from [2].	13
5.1	Survival probability in function of the distance to the detector obtained through the two-flavor approximation. Taken from reference [2].	17
6.1	Various plots showing different attributes of class <code>RingNode</code> . .	20

List of Tables

7.1 First results on geoneutrino flux (in $cm^{-2}/\mu s$) for different BSE and HPE distribution models. Using average probability from two-flavor approximation.	21
---	----

Preface

Acknowledgements

1

Introduction

“I have done something very bad today by proposing a particle that cannot be detected”

– Wolfgang Pauli

Fortunately, Pauli was a bit wrong in this one, not because of the prediction of the particle, but for the fact that we were, eventually, able to detect these particles called neutrinos. They have been proven to be some of the most bizarre mysteries of our universe due to their unique physical behavior and properties. Their low interaction and oscillation phenomena makes them, not only difficult to see, but also useful in some areas of study. The present work focus on how can we exploit these characteristics to withdraw useful information of some physically unreachable places, for example, the Earth’s interior.

In this work, I will be simulating the geoneutrino flux from an azimuthally symmetrical Earth, taking into account the PREM density model (reference [1]). This simple Earth’s structure model plus the usage of an exact solution for the antineutrino oscillation in the matter (of reference [10]) are a “simple enough” model of the problem that will allow to draw some conclusions on the Heat Producing Element distribution in the mantle and evaluate the usefulness of the complete, exact treatment of neutrino oscillations in this context.

The second chapter briefly describes the relevance of this study. Then, the distribution of radioactive elements in the Earth is discussed, first, through an overview of the Goldschmidt classification of chemical elements, and then, showing the abundances of the relevant isotopes in each of the three main layers of the planet.

In chapter 4 the phenomena of radioactivity is explained, as well as the different types of radioactive decay. The relevant decay chains are shown, along with the geoneutrino spectra for the β^- decay.

Chapter 5 is an overview of the neutrino physics. This includes a short description of the oscillation phenomena, as well as introducing two different

methods of calculating the survival probability for an electron antineutrino: the exact, three-flavor matter oscillation used in this study and the two-flavor matter oscillation used in some previous studies.

Then, in chapter 6, the details of the modeling, including some aspects of the programs written, are given. This is considered a crucial part of this work as it will be the base of any further study to be done.

The chapter 7, the results of the simulations are given, while in chapter 8 they are discussed. Chapter 9 describes what is left to be done, based on the results obtained in this study. Finally some conclusions on this project are given.

2

Relevance of the Study

The Earth is a complex system, in which we are rarely able to directly probe some characteristics, such as the composition of the deep Earth. In this aspect, one usually uses the available information in the surface, such as the composition of xenoliths, or seismic information, directly related to rheology, from which some relations to the composition can be withdrawn. Inspired by the latter, we can say that the development of indirect methods to probe the deep Earth is important, given the impossibility of directly doing it.

Neutrino geoscience is a relatively new field in geophysics and some applications of it are the estimation of radiogenic heat flux (Urey ratio) and testing HPE distributions or BSE models, nevertheless, being a new field as it is, the full potential of neutrino geoscience is yet to be discovered.

In order to develop reliable studies that involve (anti)neutrino oscillations through different variable densities, the appropriate computational tools must be developed. Thus, this study includes the development of UANDINO, the Uniandes ANtineutrINO Oscillation calculator. Which is a GSL based software dedicated to provide an exact calculation of transition and survival probabilities for an (anti)neutrino traveling through a varying density path with energy E_ν . Along with it, other side programs were developed for modeling the Earth's structure.

3

Distribution of Radioactive Elements

3.1 Distribution of Elements

A first, basic approach to understanding the distribution of elements in the Earth was given by Goldschmidt [4], who developed a classification system for the chemical elements. This classification is, in a nutshell, *lithophile* or oxygen-loving elements tend to remain in the uppermost part of the solid planet; *siderophile* or iron-loving elements, tend to be close to the nucleus and are not attracted to oxygen, unlike the lithophiles. The *chalcophile* elements are sulfur-loving and, thus, do not like the deep Earth. Finally, the *atmophile* elements are those who like to be in the atmosphere.

There are many radioactive isotopes in the Earth, which are, basically, atoms so heavy that they are unstable, and go through different processes to reach a more stable state. This will be the topic of chapter 4. Most of these heavy elements are classified as lithophiles. We are particularly interested in some isotopes that dominate the geoneutrino production (99% of production) [7], these are ^{40}K , ^{235}U , ^{238}U and ^{232}Th .

Within each of the groups given by Goldschmidt and briefly described here, there is other classification that discriminates elements based on their condensation temperature. The elements with a high value of this parameter are called *refractory* while the ones with a lower one are called *volatile*. Let us then picture the scenario of the formation of the Earth. About 4500 *Gyr* ago, the solar system and the Earth were being formed, the latter through planetary accretion, this means, a hot, undifferentiated mass of molten rock that is slowly cooling down, the consequences of this are, first of all, density differentiation, that causes the heavier elements to accumulate near the center of mass, thus, forming the nucleus. It also causes the elements to con-

dense, so the refractory ones, are quickly trapped into the Earth, making it possible to infer the initial abundances of these elements in the primitive Earth by looking at their abundances in different meteorites. On the other hand, volatile elements will not be trapped so easily or quickly, instead, there is a possibility that these elements have escaped the primitive Earth while it was hotter; the gases are extremely volatile, while there are other elements, like potassium (whose relevance will become obvious in the following sections) that are moderately volatile.

I have mentioned that the cooling down of the primitive Earth, lead to density differentiation in layers, causing the layered structure of the planet. The less-dense melt that ascended all the way up made up the crust, and is enriched in lithophile elements such as U , Th , K . Nevertheless, there is still a large amount of these elements in the mantle.

3.2 Relative Abundances

This section is devoted to discuss the different views on the distribution of the radioactive isotopes, in depth, quantitatively. There are two main discussions to be considered; first, the average composition of the Bulk Silicate Earth (BSE) and, second, the distribution of Heat Producing Elements (HPE) in the mantle.

3.2.1 Bulk Silicate Earth

In the first place, we shall define the BSE as the “average” Earth composition when excluding the nucleus, in other words, an average between mantle and crust. Three main ideas on the BSE composition have arisen through the years and each one of them relies on different, valid, arguments.

The first model is the *geochemical*, that as the name suggests, is based in geochemical arguments to give values to the abundances and abundance ratios of elements in the planet. McDonough [8] analyzed peridotite samples in order to infer the BSE average compositions. Reference [8] reports values of $A_{Th}^{BSE} = 79.5 \text{ ppb}$, $A_K^{BSE} = 240 \text{ ppm}$ and $A_U^{BSE} = 20.3 \text{ ppb}$, while reference [12] reports $A_{Th}^{BSE} = 80 \pm 13 \text{ ppb}$, $A_K^{BSE} = 280 \pm 60 \text{ ppm}$ and $A_U^{BSE} = 20 \pm 4 \text{ ppb}$ for this BSE model, note that both references are in agreement. A_X^Y stands for the abundance of element X in reservoir Y .

The second model is the *geodynamical*. This model is based on the current measurements of the Earth’s heat flow and assumes that the fraction of this heat due to radioactive decay is higher than the fraction due to secular cooling of the planet. In reference [12], the reported values of the abundances

are $A_{Th}^{BSE} = 140 \pm 14 \text{ ppb}$, $A_K^{BSE} = 350 \pm 35 \text{ ppm}$ and $A_U^{BSE} = 35 \pm 4 \text{ ppb}$. This model has particularly high values of A_X^Y due to the assumption that the majority of the flux is product of radioactivity.

The third and final model is the *cosmochemical*. It relies on the analysis of enstatite chondrites to infer the BSE composition, under the argument that this abundances specially the iron one, will easily explain the presence of the core, as explained in reference [7]. Reference [12] reports the following values relevant to this project: $A_{Th}^{BSE} = 43 \pm 4 \text{ ppb}$, $A_K^{BSE} = 146 \pm 29 \text{ ppm}$ and $A_U^{BSE} = 12 \pm 2 \text{ ppb}$.

In this study, I will compare the results for geoneutrino measurements for the different BSE models presented above.

3.2.2 Crust

The relative abundance of HPE in the crust has been the object of various studies ([5, 9, 11, 13, 14]) among which, for this project, I chose reference [5]. In this article, the authors develop a reference Earth model for the HPE, based on geochemical analysis performed on different rocks and following the CRUST 2.0 model for crustal thickness and properties. The values given are $A_U^C = 1.31_{-0.25}^{+0.29} \text{ ppb}$ and $A_{Th}^C = 5.61_{-0.89}^{+1.56} \text{ ppb}$.

3.2.3 Mantle

The abundance of isotope X in the mantle, A_X^M , is calculated from the values reported above for A_X^{BSE} and A_X^C and the mass balance [12]:

$$m_{BSE} A_X^{BSE} = m_C A_X^C + m_M A_X^M, \quad (3.1)$$

that is, the total mass of isotope X is the sum of the mass in the crust and the mantle. The mass of reservoir Y , m_Y , is calculated through integration of the mass density of the Earth given by the PREM model in reference [1], the details of the method will be given in chapter 6.

Additionally, the mantle structure is currently debated. Two of the most accepted models are the uniform mantle and the two-layer (EL-DL) mantle. The former consists in uniformly distributed HPE over the mantle, thus, the abundance in every point will be given by equation 3.1. The latter, in which EL and DL stand for enriched and depleted layer, respectively, consists in two layers of slightly different HPE abundances. The motivation for this is that the difference between the types of basalts (OIB, MORB, etc.) is thought to be caused by the differentiation of the mantle into two chemically distinct layers, an enriched layer and a depleted one, respect to lithophile elements. The enriched layer is said to constitute the lowermost

10% in mass of the bulk mantle [12]. The abundance in these two layers is also calculated using a relation similar to equation 3.1.

4

Radioactivity

4.1 Overview

Radioactivity is the phenomenon in which a parent isotope turns into a daughter isotope, with different characteristics, through the emission of a particle.

The history of radioactivity goes back to 1896, when H. Becquerel discovered that a uranium sample emitted some kind of penetrating radiation similar to the X rays (discovered earlier that year). In the following years, three different types of emissions were identified: alpha (α), beta (β) and gamma (γ). The nature of each of these emissions was identified through the years, concluding that α -particles correspond to 4He nuclei, β^\pm -particles correspond to e^\pm (electrons or positrons) and γ -particles are nothing but high energy photons.

Rutherford discovered that radioactive phenomena was linked directly with the nucleus (size $\sim 1 \text{ fm}$) of a given isotope, thus, it is an entirely quantum phenomenon.

The overall radioactive phenomena are described by a rather simple mathematical approach given the statistical behavior of the phenomena (which is a result, and evidence of how “quantum”it is). Given N parent isotopes in a sample at a given time t and assuming no more are added, the rate of decay (dN/dt) is proportional to N [6]

$$\frac{dN}{dt} = -\lambda N \quad (4.1)$$

That, upon integration becomes

$$N(t) = N_0 \exp(-\lambda t) \quad (4.2)$$

Where N_0 corresponds to the number of parent isotopes at time $t = 0$ and λ is called the decay constant and is unique for every isotope.

This simple model has been key to the use of the radioactive isotopes to, for

example, date rocks or organisms [6].

4.2 Types of radioactive decay

Let us now go deeper into the theory of the radioactivity, that is, briefly describe the different types of radioactive decays since not all of them produce antineutrinos, and these are the particles that concern this text.

4.2.1 Alpha decay

The theory of the alpha decay is rather simple. The α -particles are confined in a finite potential well (the nucleus X) and will, as expected, have a certain probability of tunneling said barrier. When this happens, the α -particle will escape and leave a “new” (daughter) nucleus X' [6]. The process may be written as



Where A is the atomic mass number, Z is the atomic number and N is the charge.

This decay involves both strong (nuclear) interactions and electromagnetic interactions since the potential well is given by confinement due to strong interaction between nucleons and the barrier has a decaying-exponential side, given by the Coulomb potential.

4.2.2 Gamma decay

Gamma decay is similar to the common electromagnetic emission due to atomic transitions, in fact, it is produced when a metastable state of an isotope decays into a more stable state through the emission of high energy photons. It should be noted that, in this case, no change in A or N is produced. These metastable states are common daughter isotopes to α and β decays.

Lifetimes for this kind of process is generally short, taking only fractions of a second to decay while some α -decaying isotopes may have half-lives of the order of 10^3 yr.

4.2.3 Beta decay

This type of decay can be considered to be more complex than the other two, as it responds to more complicated underlying physics: the weak interaction. It consists in a set of semileptonic processes (that involve both leptons and hadrons) that will be described below.

- Positive Beta decay:

$$p \rightarrow n + e^+ + \nu_e \quad (4.4)$$

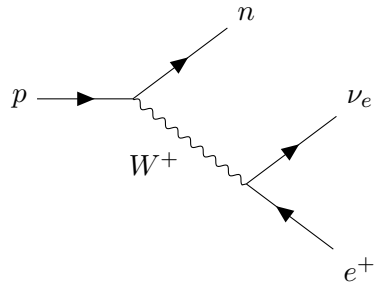


Figure 4.1: Feynman diagram for β^+ process.

- Negative Beta decay:

$$n \rightarrow p + e^- + \bar{\nu}_e \quad (4.5)$$

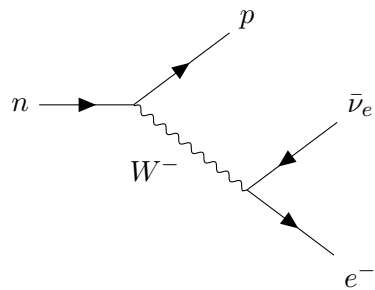


Figure 4.2: Feynman diagram for β^- process.

- Electron capture:

$$p + e^- \rightarrow n + \nu_e \quad (4.6)$$

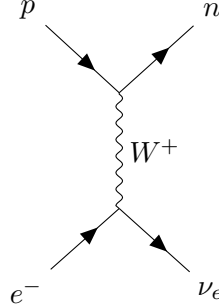


Figure 4.3: Feynman diagram for electron capture.

Note that in all these processes new particles are created in the nucleus, which is a consequence of the weak interaction that rules them.

The particles labeled with ν_e are electron neutrinos and were proposed by Pauli in order to solve the conundrum concerning the apparently continuous energy spectra of β -decay which is against the core of quantum mechanics, the inclusion of these particles in the energy spectrum of the decay made it discrete, thus, giving a solution to the problem [3].

For this project, we are strictly interested in the β^- -decay since it is the one that produces antineutrinos.

4.3 Decay Chains

Different isotopes in the Earth have decay chains that involve β^- -decay at some point, but there are a few ones that dominate the antineutrino production. The reader may have noticed that in chapter 3, I have said that the production of heat is dominated by ^{238}U , ^{232}Th and ^{40}K . Each isotope has a decay chain that includes some beta decays. These are summarized in the following equations.

$$^{238}U \rightarrow ^{206}Pb + 8\alpha + 8e^- + 6\bar{\nu}_e + 51.7MeV, \quad (4.7)$$

$$^{235}U \rightarrow ^{207}Pb + 7\alpha + 4e^- + 4\bar{\nu}_e + 46.4MeV, \quad (4.8)$$

$$^{232}Th \rightarrow ^{208}Pb + 6\alpha + 4e^- + 4\bar{\nu}_e + 42.7MeV, \quad (4.9)$$

$$^{40}K \rightarrow ^{40}Ca + e^- + \bar{\nu}_e + 1.31MeV, \quad (4.10)$$

$$^{40}K + e^- \rightarrow ^{40}Ar + \bar{\nu}_e + 1.505MeV. \quad (4.11)$$

Note that the processes shown in equations 4.10 and 4.11 have the same parent isotope, the former happens with a probability of 89.3% and the latter with the remaining 10.7%.

In equations 4.7 through 4.11, the particles $\bar{\nu}_e$ are electron antineutrinos, also called geoneutrinos, in this context.

4.4 (Anti)Neutrino emission

As seen in the previous section, naturally produced antineutrinos from beta decay are called geoneutrinos. These are produced following a given spectrum [2], shown in figure 4.4. Figure 4.4 shows that the energy domain for

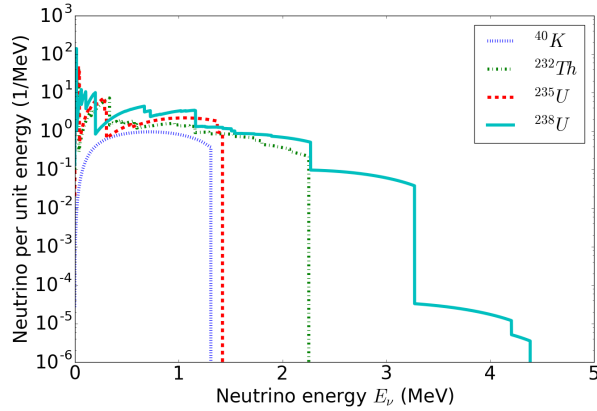


Figure 4.4: Geoneutrino energy spectrum from [2].

these particles is relatively low, this means that, in the light of reference [10], oscillations will not be of such importance because the transition or survival probabilities do not show a clear pattern in these energy scales. Nevertheless it is worth mentioning that resonances in the probabilities are present at higher energy scales.

5

Neutrino Physics

This chapter is only an overview of the special physics that surrounds these particles, for a thorough explanation you should see reference [3] and for details on time evolution, reference [10].

Neutrinos are neutral leptons that interact weakly and are always produced in a given flavor eigenstate $|\nu_\alpha\rangle$ with $\alpha = e, \mu, \tau$. In equations 4.4 to 4.6, all neutrinos are labeled ν_e that stands for electron neutrino, this is because they are all associated with the “ordinary” matter which is composed by electrons, not tauons (τ) or muons (μ), which are other charged leptons, this is, electrically charged particles that lack color charge.

I just mentioned neutrinos are produced in flavor states, but these are not mass (energy) eigenstates and, since the Hamiltonian entirely controls the time evolution of a quantum system, the neutrinos will not evolve (travel) in these states but will rather oscillate between the real mass eigenstates which, as the name suggests, do have a definite (and unknown) mass, while flavor states are just a linear combination of them. This may be written as

$$|\nu_\alpha\rangle = \sum_{a=1}^3 U_{\alpha a}^* |\nu_a\rangle \quad (5.1)$$

Here, we have labeled $|\nu_a\rangle$ the mass eigenstates, with $a = 1, 2, 3$. $U_{\alpha a}^*$ is the matrix element of the transformation matrix U^* [10].

The matrix U^* is the complex conjugate of matrix U , called Pontecorvo-Maki-Nakagawa-Sakata (PMNS) matrix, that rules the mixing of the neutrinos and can be parametrized as shown in [10]

$$U = \begin{bmatrix} C_2 C_3 & S_3 C_2 & S_2 \\ -S_3 C_1 - S_1 S_2 C_3 & C_1 C_3 - S_1 S_2 S_3 & S_1 C_2 \\ S_1 S_3 - S_2 C_1 C_3 & -S_1 C_3 - S_2 S_3 C_1 & C_1 C_2 \end{bmatrix} \quad (5.2)$$

Where $S_i \equiv \sin(\theta_i)$ and $C_i \equiv \cos(\theta_i)$. Parameters θ_i are the vacuum mixing angles. Here we have assumed there is no charge-parity (CP) phase, thus, $U = U^*$.

5.1 Time evolution

5.1.1 Three-flavor exact

According to the principles of quantum mechanics, the Hamiltonian of a system described by the ket $|\psi\rangle$ does define its time evolution according to

$$|\psi(t)\rangle = \exp(-i\hat{H}(t-t_0))|\psi(t_0)\rangle \quad (5.3)$$

In the case of the neutrinos, we know that they do not travel in flavor state but in mass states, then, we can write

$$|\nu_a(t)\rangle = \exp(-i\hat{H}_m(t-t_0))|\nu_a(t_0)\rangle \quad (5.4)$$

In this base, the Hamiltonian will be diagonal

$$\hat{H}_{m,\text{unperturbed}} = \begin{bmatrix} E_1 & 0 & 0 \\ 0 & E_2 & 0 \\ 0 & 0 & E_3 \end{bmatrix} \quad (5.5)$$

Inside matter, the Hamiltonian of the system is perturbed in the following way

$$\hat{V}_f = \mathcal{A} \begin{bmatrix} 1 & 0 & 0 \\ 0 & 0 & 0 \\ 0 & 0 & 0 \end{bmatrix} \quad (5.6)$$

Where \mathcal{A} depends on the density of the matter the neutrino is going through, and is defined as

$$\mathcal{A}(r) \approx \pm \sqrt{2} G_F \frac{\rho(r)}{m_N} \quad (5.7)$$

Here, G_F is the Fermi coupling constant, $\rho(r)$ is the matter density and m_N is the nucleon mass.

The perturbation V_f (f stands for flavor base) only affects electron-flavored neutrinos because matter, as we see it, is electronic. Taking this into account, the perturbed Hamiltonian, in mass basis is

$$\hat{H}_m = \begin{bmatrix} E_1 & 0 & 0 \\ 0 & E_2 & 0 \\ 0 & 0 & E_3 \end{bmatrix} + U^{-1} V_f U \quad (5.8)$$

Introducing equation 5.8 into 5.4 we can get the time evolution operator \hat{U}_f as follows (reference [10]). Consider a $N \times N$ matrix M , the exponential of the matrix is defined as $\exp M = \sum_{n=0}^{\infty} \frac{1}{n!} M^n$. Now, recall Cayley-Hamilton's theorem: given a matrix M , the characteristic polynomial is $p(x) = \det(x - M) = \sum_{i=0}^N c_i x^i$ ($c_N = 1$, $p(x)$ is monic), the theorem implies that $p(M) = 0$, this means that

$$p(M) = 0 = M^N + c_{N-1} M^{N-1} + \cdots + c_0, \quad (5.9)$$

then,

$$M^N = -c_{N-1}M^{N-1} - \cdots - c_0, \quad (5.10)$$

therefore, if one wishes to calculate M^m for any $m \geq N$, it will be given by

$$M^m = k_{N-1}^{(m)} M^{N-1} + \cdots + k_0^{(m)}, \quad (5.11)$$

given that coefficients $k_i^{(m)}$ are properly calculated. Knowing this, the exponential of the matrix

$$\exp M = \sum_{n=0}^{\infty} \frac{1}{n!} M^n = \sum_{n=0}^{N-1} a_n M^n \quad (5.12)$$

and this result is exact.

Then, the transition probability from an initial flavor α state to a β one will be

$$P_{\alpha \rightarrow \beta} = |\langle \beta | \hat{U}_f | \alpha \rangle|^2. \quad (5.13)$$

Given a density profile $\rho(\mathbf{r})$, one can divide it into K slices (or steps) with constant \mathcal{A} and calculate the respective time evolution operators $\hat{U}_{f,i}$ ($i = 0, \dots, K$) and build a total operator $\hat{U}_{f,total} = \prod_i \hat{U}_{f,i}$ with which total survival probability is calculated using relation 5.13.

5.1.2 Two-flavor approximation

Previous studies ([2, 7]) use the two-flavor approximation to neutrino oscillation. This takes into account that the τ neutrino is so heavy that it is rarely produced. In this case, we may write (as explained in [2])

$$\hat{H}_m = \begin{bmatrix} E_1 & 0 \\ 0 & E_2 \end{bmatrix} + U^{-1} V_f U, \quad U = \begin{bmatrix} \cos \theta & \sin \theta \\ -\sin \theta & \cos \theta \end{bmatrix}, \quad (5.14)$$

This results in a perturbed hamiltonian of the form

$$\hat{H}_f = \begin{bmatrix} -\frac{\Delta m^2}{4E_\nu} \cos 2\theta + \mathcal{A} & \frac{\Delta m^2}{4E_\nu} \sin 2\theta \\ \frac{\Delta m^2}{4E_\nu} \sin 2\theta & \frac{\Delta m^2}{4E_\nu} \cos 2\theta \end{bmatrix} \quad (5.15)$$

In order to solve this matter oscillation case, a new U' matrix is proposed

$$U' = \begin{bmatrix} \cos \theta' & \sin \theta' \\ -\sin \theta' & \cos \theta' \end{bmatrix}, \quad (5.16)$$

where

$$\cos 2\theta' \equiv \frac{-2\mathcal{A}E_\nu/\Delta m^2 + \cos 2\theta}{\sqrt{(2\mathcal{A}E_\nu/\Delta m^2 - \cos 2\theta)^2 + \sin^2 2\theta}}, \text{ and} \quad (5.17)$$

$$\sin 2\theta' \equiv \frac{\sin^2 2\theta}{\sqrt{(2AE_\nu/\Delta m^2 - \cos 2\theta)^2 + \sin^2 2\theta}} \quad (5.18)$$

Then, the mass difference is

$$\Delta m'^2 = \sqrt{(2AE_\nu - \Delta m^2 - \cos 2\theta)^2 + (\Delta m^2)^2 \sin^2 2\theta}. \quad (5.19)$$

This theorem is the basis of the whole calculation \hat{U}_f , for the rest of the algebra, you should check reference [10].

The probability is then calculated as shown in 5.13 if one defines $\hat{U} = \exp(i\hat{H}t)$. This results in

$$P_{ee} = 1 - \sin^2 2\theta' \sin^2 \left(\frac{\Delta m'^2 L}{4E_\nu} \right), \quad (5.20)$$

where L is the traveled distance (with constant A). These references argue that this probability is well averaged since the quantity $L_{osc} = \pi \frac{4E_\nu}{\Delta m^2} \ll R$ (so $\sin^2(\dots) = 0$, L_{osc} is therefore known as oscillation distance), this results in very “tight” oscillations (as illustrated in figure 5.1), for all paths in the Earth. Then,

$$\langle P_{ee} \rangle = 1 - \frac{1}{2} \sin^2 2\theta' = 0.55. \quad (5.21)$$

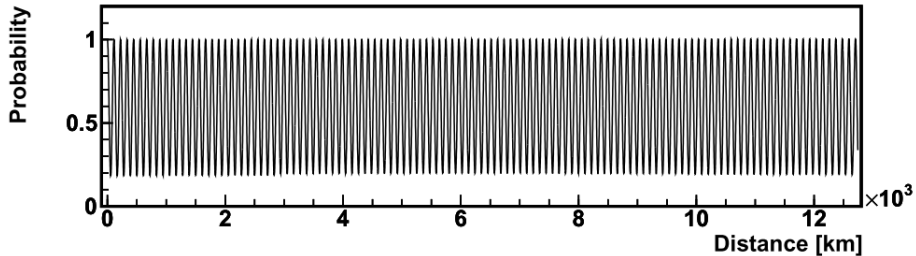


Figure 5.1: Survival probability in function of the distance to the detector obtained through the two-flavor approximation. Taken from reference [2].

On this project, I will adopt the exact solution to evaluate the real effect of a varying electron-density in the (anti)neutrino oscillation phenomena and how it will affect the detection.

6

The Model

6.1 Modelling the Earth

In order to model the Earth, different assumptions were made. The biggest one is, probably, that the Earth is azimuthally symmetrical, nevertheless the model to be shown will allow for some complex radial and polar asymmetries.

All programs developed for the project are available in the repository ¹ dedicated to it. Implementation is mainly done in C++, but a small part involving the probability calculations is done in Python.

For integrating, I use cylindrical coordinates, in which the z coordinate is, as usual $z \in [-R, R]$, where $R = 6371\text{km}$ is Earth's Radius. The radial coordinate is called $x \in [0, \sqrt{R^2 - z^2}]$. Thus, we divide the Earth in rings, or nodes each ring will have a volume $dV = 2\pi x dx dz$. Computationally, the Earth is modeled by a 500×1000 matrix of instances of the class `RingNode`, this type of data has a variety of attributes that will be introduced when necessary in this text.

The matrix itself is an attribute of the class `Planet`, that holds other attributes such as total mass, volume and fluxes. Figure 6.1 shows different attributes of `RingNode` class. These classes are defined in `earth_simul.h` and the respective implementation file `earth_simul.cpp`.

6.2 Modelling the Flux

6.2.1 The Flux Integral

As in reference [12], the flux is given by the integral of equation 6.1.

$$\Phi_X(\mathbf{r}) = \frac{n_X \lambda_X}{4\pi} \int_{\Omega} \int_{\oplus} \frac{a_X(\mathbf{r}') \rho(\mathbf{r}') P_{ee}(\mathbf{r} - \mathbf{r}', E_\nu)}{|\mathbf{r} - \mathbf{r}'|^2} d^3 r dE_\nu \quad (6.1)$$

¹https://github.com/dforero0896/Physics_Monograph

Here, n_X stands for the number of neutrinos produced in decay chain X (from equations 4.7 through 4.11), λ_X is the decay constant for each chain, a_X is the isotopic abundance at position \mathbf{r}' , ρ is the matter density and P_{ee} is the survival probability of the geoneutrinos produced at \mathbf{r}' with energy E_ν , travelling towards \mathbf{r} . Finally, the factor $\frac{1}{4\pi|\mathbf{r}-\mathbf{r}'|^2}$ accounts for the spherically divergent flux. Integration should be done in domains \oplus (Earth) spatially and Ω , shown in figure 4.4, for the energy. All these quantities are attributes to the class `RingNode`.

6.2.2 Survival Probability

The quantity P_{ee} depends on both the path ($|\mathbf{r} - \mathbf{r}'|$) the geoneutrino takes, and the energy (E_ν) with which it is produced. The energy of these antineutrinos depends on the spectra ($\frac{dn}{dE_\nu}$) in figure 4.4. The way of performing the integral over the energies is the following: for a given node in the matrix, the path to the detector is calculated, for this path and $M = 300$ samples of energy, the survival probability (P_i) is obtained. Then, for the same energies, the spectra is sampled, this results in M values f_i . Each is normalized as $w_i = f_i / \sum_i f_i$. These w_i are the weights corresponding to each probability. Finally the probability for each node is

$$P_{ee}(|\mathbf{r} - \mathbf{r}'|) = \sum_i w_i P_i. \quad (6.2)$$

There are three programs that handle this step: `raw_probs.cpp` that calculates the raw probabilities (as previously mentioned in section 5.1.1) for a node and writes them in the file `raw_probs.csv`, `prob_weight.cpp` that calculates the weights w_i for a node and exports them to a file `prob_weight.dat` and `prob_integrating.py` that is in charge of running the C++ programs for all node i, j in the Earth and calculating the “average” probability for each one (equation 6.2) and writing them to file `probability_planet.csv`, which is used in the calculations of the flux.

It is worth mentioning that prior studies use an average probability given by approximating the two-flavor oscillation model (equation ??).

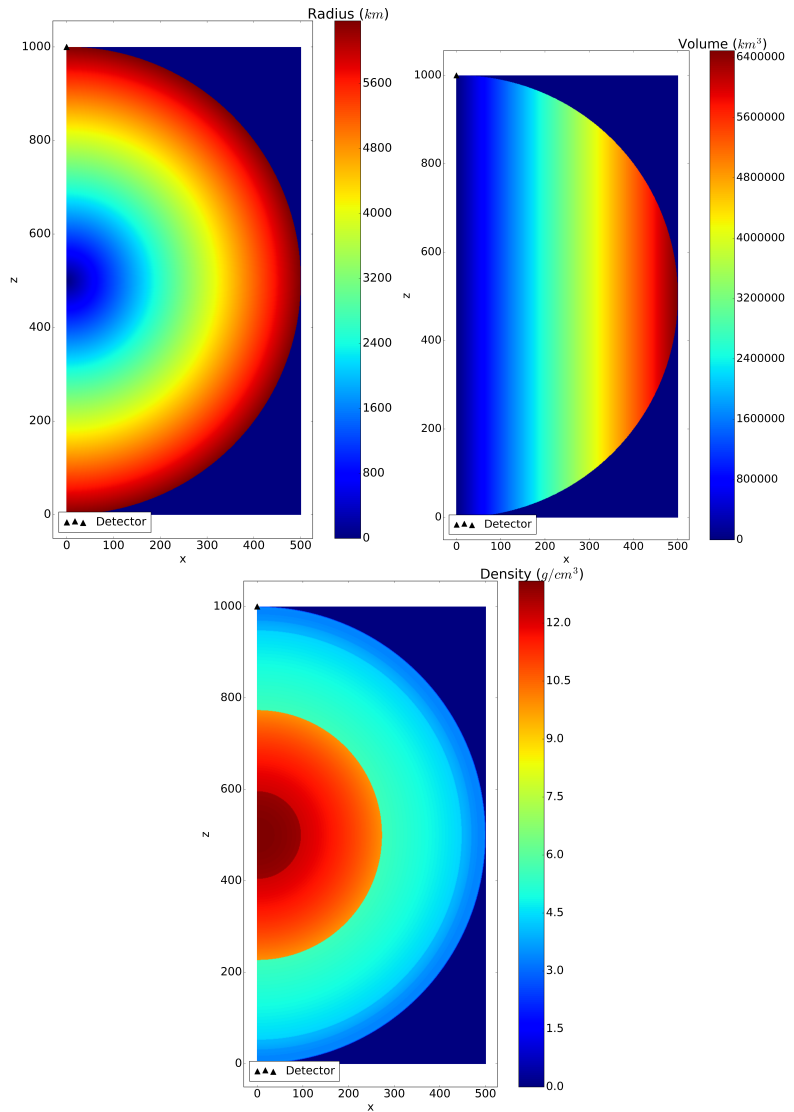


Figure 6.1: Various plots showing different attributes of class `RingNode`.

7

Results

Following the work in reference [12], a test with an average survival probability (from reference [7]) of $\langle P_{ee} \rangle = 0.55$ from the two-flavor approximation, the different HPE distributions and BSE models was done, the results are shown in table 7.1. The simulation allows for an inspection on the distribu-

BSE Model \HPE distribution	Uniform		Two-layer	
	Φ_U	Φ_{Th}	Φ_U	Φ_{Th}
Geochemical	0.626	0.526	0.530	0.436
Cosmochemical	0.242	0.139	0.236	0.140
Geodynamical	1.345	1.158	1.079	0.917

Table 7.1: First results on geoneutrino flux (in $cm^{-2}/\mu s$) for different BSE and HPE distribution models. Using average probability from two-flavor approximation.

tion of the flux, figure ?? shows the flux contribution to the total for both isotopes.

8

Analysis

9

Further Problems

10

Conclusions

References

- [1] Adam M. Dziewonski and Don L. Anderson. “Preliminary reference Earth model”. In: *Physics of the Earth and Planetary Interiors* 25.4 (1981), pp. 297–356. ISSN: 00319201. DOI: 10.1016/0031-9201(81)90046-7.
- [2] S. Enomoto. “Neutrino Geophysics and Observation of Geo-Neutrinos at KamLAND”. PhD thesis. 2005, p. 233.
- [3] Carlo Giunti and Chung W. Kim. “Fundamentals of Neutrino Physics and Astrophysics”. In: *Fundamentals of Neutrino Physics and Astrophysics* (2010), pp. 1–728. ISSN: 0717-6163. DOI: 10.1093/acprof:oso/9780198508717.001.0001. arXiv: 9809069v1 [arXiv:gr-qc].
- [4] Victor Goldschmidt. *Geochemistry*. 1st ed. The Clarendon Press, 1958.
- [5] Yu Huang et al. “A reference Earth model for the heat-producing elements and associated geoneutrino flux”. In: *Geochemistry, Geophysics, Geosystems* 14.6 (2013), pp. 2003–2029. ISSN: 15252027. DOI: 10.1002/ggge.20129. arXiv: 1301.0365.
- [6] Kenneth S. Krane. *Introductory Nuclear Physics*. Wiley, 1988. ISBN: 9780471805533. DOI: 9780471805533.
- [7] L. Ludhova and S. Zavatarelli. “Studying the earth with geoneutrinos”. In: *Advances in High Energy Physics* 2013 (2013). ISSN: 16877357. DOI: 10.1155/2013/425693. arXiv: 1310.3961.
- [8] Shen-Su McDonough, William F; Sun. “The Composition of The Earth”. In: *Chemical Geology* 120 (1995), pp. 223–253. ISSN: 00092541. DOI: 10.1016/0009-2541(94)00140-4.
- [9] Scott M. McLennan. “Relationships between the trace element composition of sedimentary rocks and upper continental crust”. In: *Geochemistry, Geophysics, Geosystems* 2.4 (Apr. 2001), n/a–n/a. ISSN: 15252027. DOI: 10.1029/2000GC000109. URL: <http://doi.wiley.com/10.1029/2000GC000109>.

- [10] Tommy Ohlsson and Hakan Snellman. “Neutrino oscillations with three flavors in matter of varying density”. In: *The European Physical Journal C* 20.3 (2001), pp. 507–515. ISSN: 1434-6044. DOI: 10.1007/s100520100687. arXiv: 0103252 [hep-ph]. URL: <http://arxiv.org/abs/hep-ph/0103252%7B%5C%7D5Cnhttp://www.springerlink.com/index/10.1007/s100520100687>.
- [11] R.L. Rudnick and S. Gao. “3.01 Composition of the Continental Crust”. In: *Treatise on Geochemistry*. 2003, pp. 1–64. ISBN: 9780080437514. DOI: 10.1016/B0-08-043751-6/03016-4. URL: <http://www.sciencedirect.com/science/article/pii/B0080437516030164>.
- [12] Ondrej Sramek et al. “Geophysical and geochemical constraints on geoneutrino fluxes from Earth’s mantle”. In: *Earth and Planetary Science Letters* 361 (2013), pp. 356–366. ISSN: 0012821X. DOI: 10.1016/j.epsl.2012.11.001. arXiv: <arXiv:1207.0853v2>.
- [13] Stuart Ross Taylor and Scott M. McLennan. “The geochemical evolution of the continental crust”. In: *Reviews of Geophysics* 33.2 (May 1995), p. 241. ISSN: 8755-1209. DOI: 10.1029/95RG00262. URL: <http://doi.wiley.com/10.1029/95RG00262>.
- [14] K Hans Wedepohl. “The composition of the continental crust”. In: *Geochimica et Cosmochimica Acta* 59.7 (Apr. 1995), pp. 1217–1232. ISSN: 00167037. DOI: 10.1016/0016-7037(95)00038-2. URL: <http://www.sciencedirect.com/science/article/pii/0016703795000382>.

Index

Bulk Silicate Earth (BSE)

- cosmochemical, 8
- geochemical, 8
- geodynamical, 8

Eigenstate

- flavor, 15
- mass, 15

Goldschmidt

- classification, 7

Hamiltonian, 15

Neutrino

- definition, 15